

Comprehensive Status Report: November 18, 2004

OTRC Project Title: Suction Caissons & Vertically Loaded Anchors  
MMS Project 362 TO 16169  
Project Subtitle: Suction Caissons & Vertically Loaded Anchors: Design Analysis Methods  
PI's: Charles Aubeny & Don Murff  
MMS COTR: A. Konczvald

This report provides a comprehensive summary of the research completed in all prior Phases of this project (September 1999 – August 2004), and describes research being done in the present Phase (September 2004 – August 2005) to complete this project.

Note that this report addresses one of four related research areas on this project. The other three areas are reported separately under the subtitles – Suction Caissons: Model Tests, Suction Caissons: Seafloor Characterization for Deepwater Foundation Systems, & Suction Caissons: Finite Element Modeling.

# Suction Caissons & Vertically Loaded Anchors: Design Analysis Methods

**Charles Aubeny and Don Murff**

## **PROJECT OBJECTIVES**

The project objectives are to (1) determine the currently available best practices for analysis and design of suction caisson anchors (SCA's) and vertically loaded anchors (VLA's) including drag embedment anchors, and (2) effect improvements in the installation and capacity predictions for SCA's and VLA's.

The overall research program for investigating anchor performance includes experimental model tests, finite element analyses, and developing simplified design tools for practitioners. This portion of the project focused on simplified design tools for estimating the ultimate pullout loads of suction anchors.

## **PROGRESS AND RESULTS – SUCTION ANCHORS**

### **General Methodology**

The general framework for development of the simplified formulations discussed herein is plastic limit analysis (PLA). PLA formulations can include upper and lower bound solutions. This research largely utilized an upper bound approach involving:

1. Postulating a kinematically admissible collapse mechanism.
2. Computing the rate of internal energy dissipation associated with that mechanism.
3. Equating the rate of internal energy dissipation to the rate of work due to externally applied loads to determine an upper bound estimate of load capacity.
4. Systematically optimizing the collapse mechanism to obtain a least upper bound estimate of load capacity.

### *Internal Energy Dissipation*

The second step in the upper bound analyses involves evaluating the rate of internal energy dissipation associated with the postulated collapse mechanism. In the most rigorous approach, this involves four steps. First, strain rates at any point in the deforming soil surrounding the suction anchor are calculated by taking spatial derivatives of velocity fields. Next, the corresponding stresses at any point in the soil mass are calculated by invoking a flow rule – associated flow rules in the case of the formulations considered in this paper. The product of strain rate and stress yields the rate of energy dissipation per unit volume. The total rate of energy dissipation is calculated by integrating –usually numerically - over the appropriate volume. Discontinuous velocity fields can also be accommodated in the analysis. Although strain rates across a slip plane are infinite, the rate of energy dissipation per unit surface area approaches a finite value as the volume of soil containing the slip plane becomes infinitesimally thin (Murff, 1980). In this case, the dissipation energy per unit area is integrated across the surface area of the slip plane.

The analysis described above can require considerable computational effort, as it requires evaluation of volume and surface integrals that can involve considerable complexity when three dimensional collapse mechanisms are considered. Further, even when simplifying assumptions are made regarding the collapse mechanism, optimizing the geometry of the mechanism to achieve a least upper bound solution is a complex problem in itself. In the case of the Murff and Hamilton (1993) analysis to be discussed subsequently, four optimization parameters are utilized in the search for a least upper bound solution for lateral load capacity. Considerable simplification of the PLA analysis is possible if the net effect of the three-dimensional stress field in the soil surrounding the caisson is expressed in terms of equivalent forces and moments acting on the caisson. This expedient greatly reduces the computational effort in evaluating the rate of energy dissipation – the dimension of the integrals reduces from three to one – and reduces the number of optimization variables describing the collapse mechanism. The resulting reduction in computational effort permits analyses that are well within the capabilities of spreadsheet programs, although the range of site conditions that can be considered by this simplified approach is more restrictive than the more rigorous solution methods.

The simplified analyses described above use a generalized plastic limit analysis (Prager, 1959) in which forces and moments are considered as ‘generalized stresses’, with velocities and rotation rates being the corresponding work conjugate ‘generalized strains’. In addition, for the case of suction anchors subjected to inclined loads, the interaction relationships between horizontal, vertical, and moment resistance can be considered as a generalized yield surface. Therefore, by invoking an associated flow rule, velocities and rotation rates can be related to resisting forces and moments in the same manner that strain rates are related to stresses in conventional plasticity analyses.

#### *PLA of a Laterally Loaded Suction Caisson*

Figure 1 shows the starting point for this research, the collapse mechanism postulated by Murff and Hamilton (1993) for laterally loaded piles which is equally applicable to laterally loaded suction anchors. The mechanism comprises three regions: a surface failure wedge, a zone at depth in which the soil flows horizontally around the translating-rotating caisson, and a spherical failure surface at the caisson tip. Murff and Hamilton show that this collapse mechanism can be fully described in terms of four optimization

parameters describing the rotation of the caisson ( $L_0$ ) and the geometry and motions of the surface failure wedge. The optimal combination of these parameters leads to a least upper bound solution for suction anchor lateral load capacity. Lateral resistance calculated from the Murff-Hamilton approach compare favorably to the empirical relations of Matlock (1970) and Reese et al. (1975).

A substantial portion of this research involved simplification and modifications to the Murff-Hamilton solution to develop (1) a simplified solution for laterally loaded suction anchors, (2) a model for suction anchors subjected to combined vertical and horizontal loads, and (3) a model for suction anchor capacity in anisotropic soils.

## Laterally Loaded Suction Caissons

### *Model Development*

The Murff-Hamilton mechanism described above offers an effective but somewhat computationally intensive approach for estimating suction anchor lateral load capacity. In seeking a simpler design tool, an equivalent mechanism in Figure 2 was proposed for this research (Aubeny et al., 2000). The horizontal soil force per unit of caisson depth  $H(z)$  is calculated from an empirical expression for side resistance proposed by Murff and Hamilton (1993) based on their analysis of the collapse mechanism in Figure 1. The important outcomes of this simplification are: (1) the computations involved in evaluating internal energy dissipation are greatly reduced, and (2) the collapse mechanism involves only a single optimization variable ( $L_0$ ), greatly simplifying the

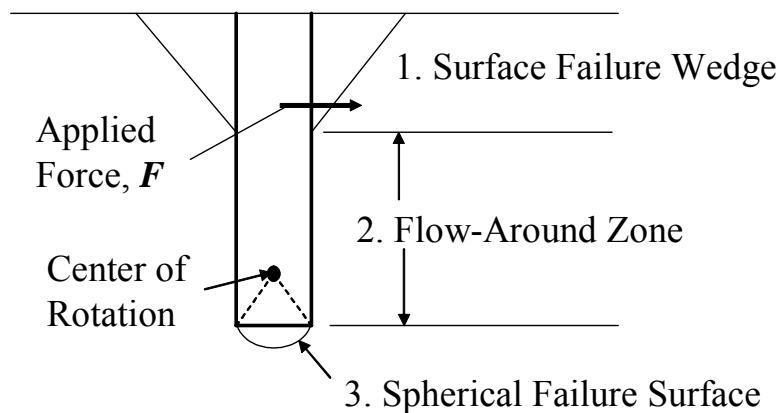
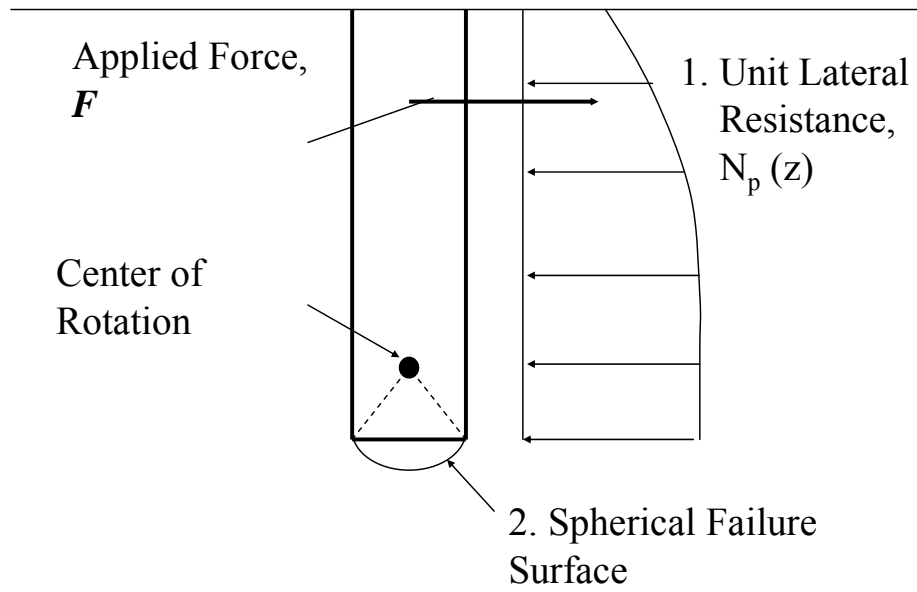


Figure 1. Failure Mechanism Assumed by Murff and Hamilton (1993)



**Figure 2.** Simplified Analysis by Aubeny et al. (2001)

process of seeking a least upper bound. The simplified framework presented above permits solution in a spreadsheet format.

### *Parametric Studies*

Using the simplified analyses, the PI's investigated the influence of a number of parameters on lateral load capacity of suction anchors, including anchor-line attachment depth, caisson aspect ratio, soil strength profile characteristics, adhesion conditions at the soil-caisson interface, and the possible occurrence of a gap at the soil-caisson interface on the windward side of the caisson. A comprehensive parametric study is given by Aubeny et al. (2001). It should be noted that a model based on mechanics principles such as this allows such studies, whereas empirical models do not.

An example of the computer program's capabilities is given in Figure 3. The analysis considers the hypothetical case of a 60-ft long by 15-ft diameter caisson in a soil having an undrained shear strength of 50 lb/ft<sup>2</sup> at the mudline and increasing at a rate of 10 lb/ft<sup>2</sup> at per foot of depth. The analyses illustrate the importance of load attachment depth, with the lateral load capacity at the optimal attachment depth exceeding that at the mudline by a factor of about 4. In this case the optimal attachment depth is at about three-fourths of the caisson depth. The adhesion condition at the soil-caisson interface is of moderate significance, with the load capacity for a rough interface exceeding that for a smooth interface by up to 25%.

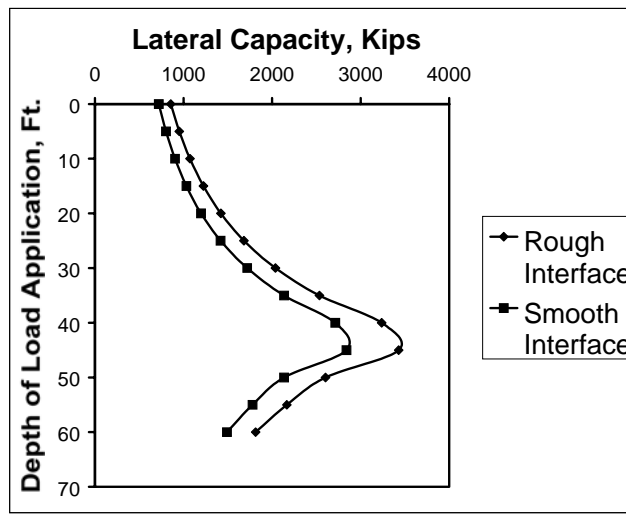
### **Suction Caissons under Inclined Loading**

Using an approach originally proposed by Randolph (2001), the simple model of a rotating pile or caisson can be extended to conditions of inclined loading as shown in Figure 4. If  $v_0$  is the lateral virtual velocity at the mudline, the axial velocity of the anchor,  $v_a$ , can be expressed as a ratio of this virtual velocity  $v_a = \xi v_0$ , where  $\xi$  is an optimization parameter. As described earlier for laterally loaded anchors, the lateral velocity at any point on the side of the caisson can be expressed in terms of the virtual velocity at the mudline,  $v_0$ , and the optimization parameter,  $L_0$ . Hence, the problem of inclined load capacity of a suction anchor can be formulated in terms of two optimization parameters, the depth to the center of rotation,  $L_0$ , and the ratio of vertical to lateral velocity at the mudline,  $\xi$ . While the additional optimization parameter increases the complexity of the analysis somewhat, the computations are still well within the capabilities of spreadsheet calculations on a personal computer; therefore, the formulation described herein can be used as a practical design tool. Details of the formulation are given by Aubeny et al. (2003a) and Aubeny and Murff (2003). Key steps in the formulation are summarized below.

### *Side Resistance Interactions*

A key component of the formulation for inclined loading involves the interactions between lateral and axial soil resistance acting on the sides of the caisson, resistance which is conveniently characterized by lateral and axial dimensionless bearing factors,  $N_{ps}$  and  $N_{ps}$ , respectively. The interaction between these bearing factors was evaluated through finite element analyses of a suction anchor, for which collapse loads were

determined for various directions of translation ranging from purely horizontal to purely vertical. The shape of the interaction diagram is a function of depth. Figure 5



Lateral Capacity of a Suction Caisson vs. Depth of Load Application

( $L=60$  ft.,  $D=15$  ft.,  $s_{uo}=50$  psf,  $s_{ul}=10$  psf/ft.)

Figure 3. Example of Simplified Analysis of Laterally Loaded Caisson

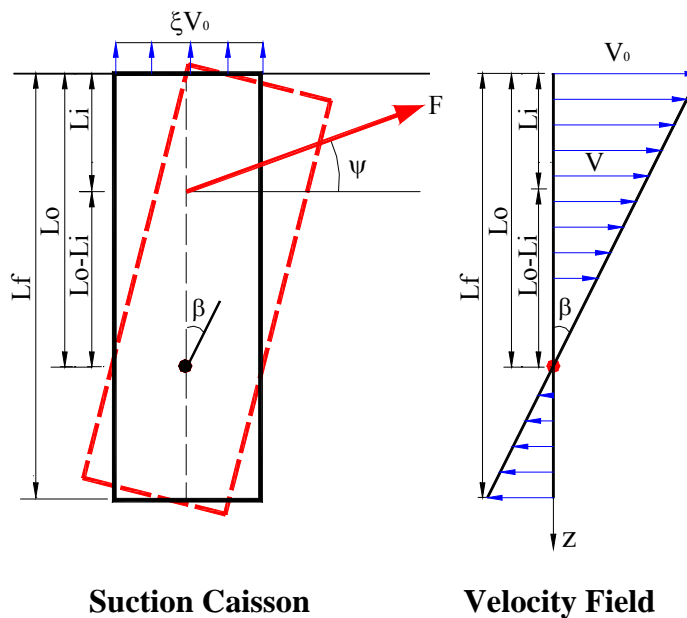


Figure 4. Deformation Mode for Caisson Subjected to Inclined Loading

shows an example interaction diagram corresponding to a point on the caisson corresponding to “deep” conditions; i.e. sufficient far from the mudline for free surface effects to be negligible.

### *Tip Resistance Interactions*

Resistance at the tip of the caisson is comprised of vertical, horizontal, and moment resistance components. Based on a “scoop” mechanism, Bransby and Randolph (1998) proposed a relationship for “skirted” foundations subject to uplift loads that characterizes the interaction between all components of resistance. In this research, Aubeny et al. (2003a) proposed the simpler “circular” interaction relationship illustrated in Figure 6. Note that the terms  $V_0$  and  $M_0$  in Figure 6 denote the maximum vertical load capacity and moment resistance for conditions of pure vertical loading and pure rotation, respectively.

### *The Upper Bound Plasticity Framework*

In the upper bound calculation discussed herein, the interaction diagrams in Figures 5 and 6 play a role directly analogous to that of the yield surface in classical plasticity theory. As an example, a determination of the internal energy dissipation due to soil resistance on the sides of the caisson would proceed according to the following steps:

1. For a given pair of optimization parameters  $L_0$  and  $\xi$  (Figure 4), kinematic considerations fully define the axial and lateral components of velocity at any depth  $z$  on the side of the caisson,  $v_a$  and  $v_l$ .
2. The associated flow law dictates that the velocity vector  $(v_a, v_l)$  be normal to the interaction diagram in Figure 5. The point on the diagram at which this condition is satisfied, establishes the appropriate bearing factors  $N_{as}$ ,  $N_{ps}$  at any depth  $z$ .
3. These bearing factors are applied to the following expression for

$$\dot{D}_s = \int (\alpha N_{as} S_u D v_a + N_{ps} S_u D v_l) dz \quad (\text{Eq. 1})$$

where  $\dot{D}_s$  is internal energy dissipation,  $\alpha$  is an adhesion factor at the soil-caisson interface,  $S_u$  is local soil undrained shear strength, and  $D$  is caisson diameter.

Calculations for vertical and moment resistance at the caisson tip using Figure 6 follow an identical sequence.

### *Parametric Studies*

Examples of suction caisson load capacity interaction diagrams for a caisson with aspect ratios  $L_f/D = 2, 6, \text{ and } 10$  in a uniform strength profile are given in Figure 7. In these examples, the caisson is rough (adhesion factor  $\alpha = 1$ ) and no gap is assumed on the windward side of the caisson. Aubeny et al. (2003a) give a comprehensive parametric study of inclined load capacity of suction caissons based on this procedure. Interaction diagrams have been developed for other conditions including non-uniform strength profiles (Aubeny et al., 2003a) and adhesion factors  $\alpha$  less than unity (Aubeny et al., 2003b).

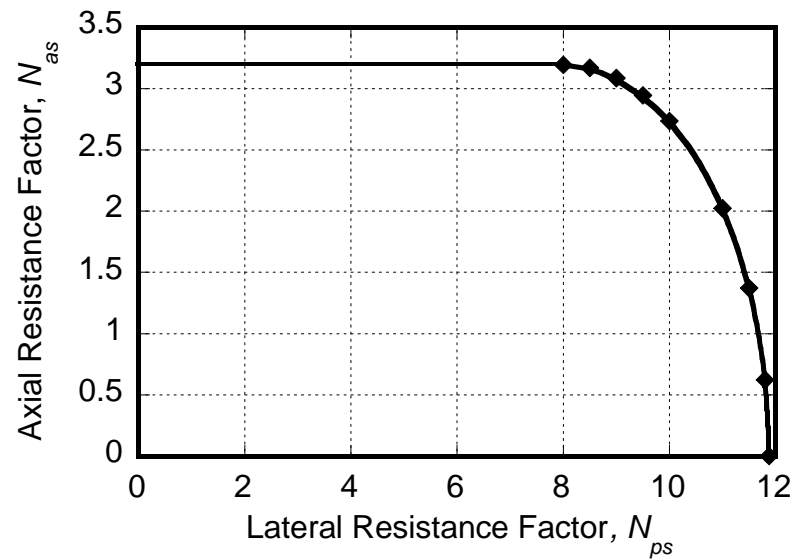


Figure 5. Axial-Lateral Caisson Side Resistance Interaction for 'Deep' Conditions

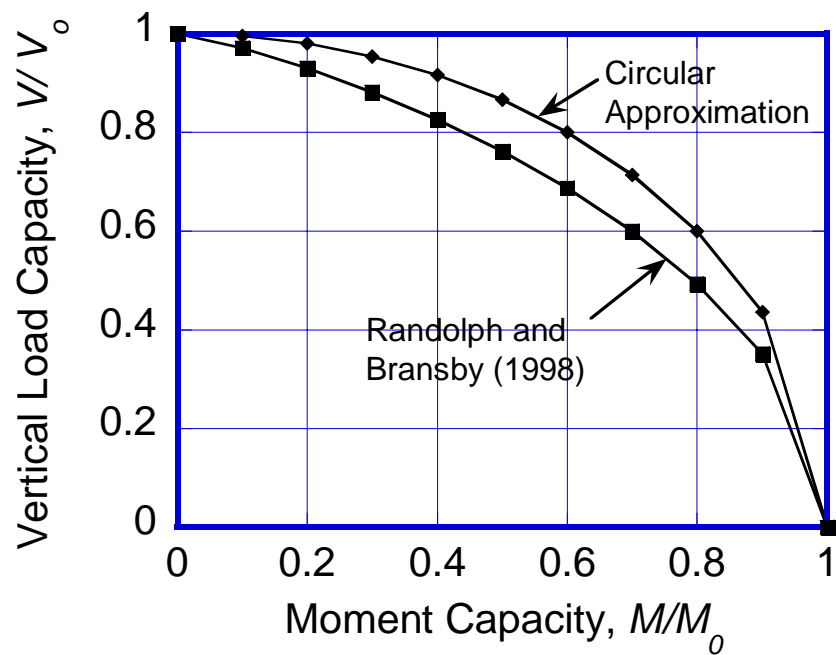


Figure 6. Axial-Rotational Caisson Tip Resistance Interaction



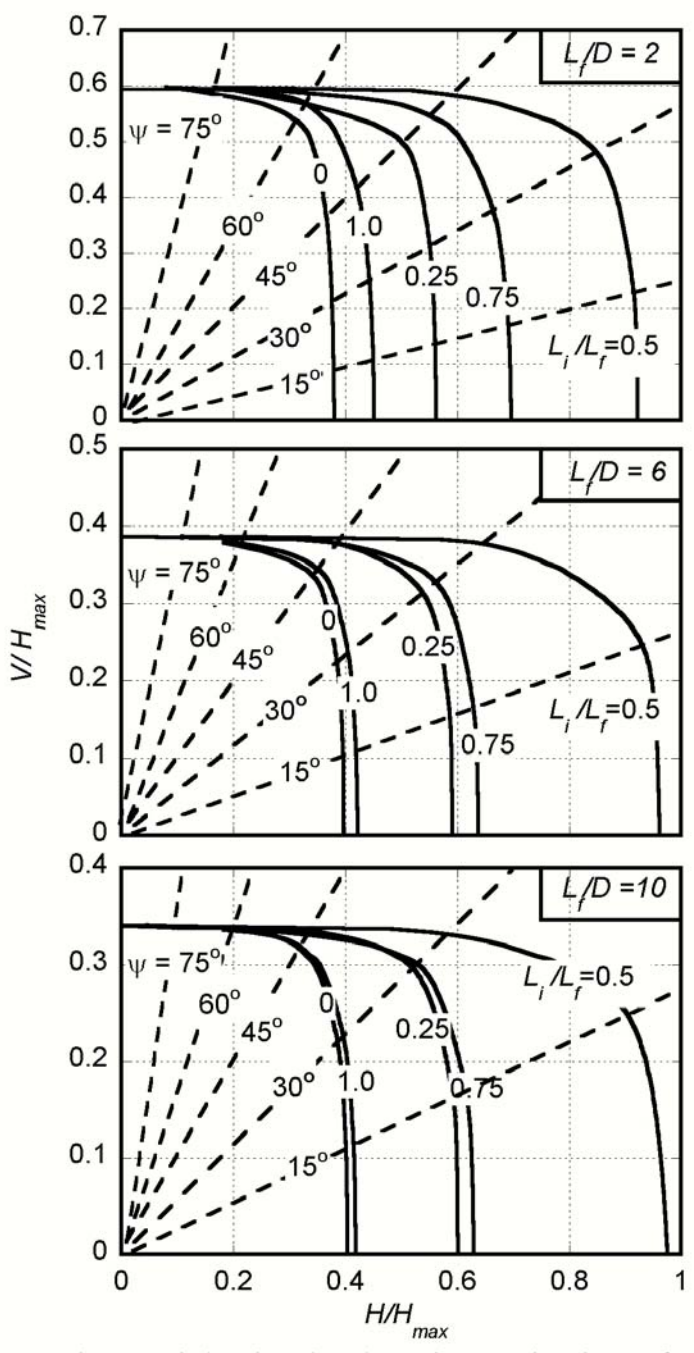


Figure 7. Caisson Inclined Load Capacity in Uniform Soil Strength Profile

### **Influence of Soil Strength Anisotropy**

The suction anchor load capacity predictions presented above assume isotropic strength properties for the clay. In actuality, the anisotropic strength properties of clays are well-established. A study was therefore directed toward investigating the effects of strength anisotropy on suction anchor load capacity predictions.

#### *Clay Strength Anisotropy*

The studies focused on  $K_0$  consolidation conditions. In this case, the relevant shearing conditions become triaxial compression, triaxial extension, simple shear, and pressuremeter (cavity expansion) shear. The undrained simple shear strength  $S_{uDSS}$  typically represents an “average” of triaxial compression and extension conditions. Hence,  $S_{uDSS}$  is typically considered the most appropriate strength measure to use in an isotropic analysis, and it provides a useful reference measure for assessing the effects of anisotropy. Data by Ladd (1991) show the strength in triaxial compression to exceed that in simple shear by a factor  $S_{uTC}/S_{uDSS} = 1.04-1.56$ , while typical data for triaxial extension indicate a range  $S_{uTE}/S_{uDSS} = 0.55-0.96$ . Limited test data on the pressuremeter shearing mode (Wood, 1981; O’Neill, 1985; Whittle and Aubeny, 1993) suggest  $S_{uPM}/S_{uDSS} = 1$ .

#### *Anisotropic Plasticity Model*

To simulate the behavior described above, this research adopted an anisotropy model proposed by Hill (1950), which was modified to specify different yield surfaces for triaxial compression and extension. Figure 8 contrasts the modified Hill model to the von Mises model used in the isotropic analyses. Also shown is an elliptical yield surface originally proposed by Davis and Christian (1971).

The modified Hill yield model was incorporated into the original Murff and Hamilton (1993) three-dimensional model for a laterally loaded pile. Derivation of the internal energy dissipation relationships for continuously deforming regions followed the approach presented by Murff (1978). The Murff-Hamilton pile failure mechanism also contains discrete slip planes. This research developed expressions for internal energy dissipation along a slip plane in an anisotropic material by modifying expressions developed earlier by Murff (1980) applicable to isotropic materials.

#### *Parametric Studies*

To assess the effects of anisotropy on suction anchor lateral load capacity, plastic limit analysis predictions were made for the 4 cases of anisotropic undrained shear strength conditions listed in Table 1. It should be noted that for the von Mises (isotropic) yield condition,  $S_{uTC}/S_{uDSS} = S_{uTE}/S_{uDSS} = 0.87$ . Predictions were made with and without a gap being assumed to form at the soil-caisson interface on the windward side of the anchor.

Table 1. Strength Parameters Considered in Parametric Study

Case	$S_{uTC}/S_{uDSS}$	$S_{uTE}/S_{uDSS}$
A	1.33	0.96
B	1.33	0.55
C	1.04	0.96
D	1.04	0.55

Figure 9 indicates that the isotropic load capacity predictions deviate from the more rigorous anisotropic predictions by no more than 10%. For conditions of no gap formation, anisotropy effects were most significant for short, squat caissons, having aspect ratios less than 6. When a gap forms on the windward side of the caisson, anisotropy affects load capacity at all anchor aspect ratios, but the anisotropic analysis predictions still deviate from the isotropic analyses by no more than 10%. Overall, it was concluded from this study that the effect of strength anisotropy on suction anchor capacity is relatively modest. However, the database on undrained strength anisotropy is relatively limited, and anisotropic conditions outside the range of that considered in the study may well be possible. Hence, the potential influence of strength anisotropy should not be entirely discounted. Full details of the anisotropy study, including comparisons to finite element studies, are documented by Aubeny et al. (2003c).

### **Model Evaluation**

Plastic limit analysis predictions of suction anchor load capacity have been validated at TAMU through comparisons to centrifuge model tests (Clukey et al., 2003) and finite element analyses (Anderson et al., 2003). Single gravity model tests of suction anchors subjected to general loading have also been performed at the University of Texas (UT). Preliminary evaluation of the UT data indicates favorable comparison to the OTRC plasticity model predictions (Rauch, 2003).

#### *Centrifuge Test Data*

Centrifuge model tests performed at the C-CORE testing facility (Clukey and Phillips, 2002) were compared to load capacity predictions from the TAMU plasticity model in a study documented by Clukey et al. (2003). Seven centrifuge tests were performed in soil conditions approximating normal consolidation for load inclination angles ranging from 24 to 90 degrees from horizontal. The soil strength profiles in the centrifuge tests were estimated from (1) piezocone tests, and (2) simple shear tests used in conjunction with the SHANSEP normalization procedure. Plastic limit analyses were performed using the best estimate of the soil strength profiles to obtain anchor load capacity predictions corresponding to the conditions of the centrifuge tests. The caisson anchors used in the tests had aspect ratios (depth/diameter) in the range 4.7-4.9, with the pad-eye located at about two-thirds of the caisson depth. Direct measurements of the soil-caisson adhesion factor  $\alpha$  were not made for these particular tests; however, based on experience, a range  $\alpha = 0.7$  to 1.0 was considered.

Figure 10 shows the comparisons between analyses and measurements. Overall, the agreement was considered quite good considering the uncertainties in the soil strength profile. Particularly noteworthy was the agreement between model and measurement with regard to the load inclination angle at which interaction effects develop; i.e., the region in which the vertical-horizontal load capacity diagram is curved. Figure 10 shows that both theory and measurement show that interaction effects occur for load attachment angles less than 40-45 degrees from horizontal. It should be noted that the interaction relationship between vertical and horizontal load capacity shown in Figure 10 is unique to the particular conditions of the tests. The plasticity model predictions (Figure 7) indicate that the characteristics of the interaction diagram are sensitive to both caisson aspect ratio and load attachment depth.

### *Finite Element Analyses*

A comprehensive study on deepwater anchors by Anderson et al. (2004) included comparisons between simplified analysis methods and more rigorous finite element predictions of suction anchor load capacity. The study considered short ( $L_f/D = 1.5$ ) and slender ( $L_f/D = 5$ ) caissons in normally and lightly over-consolidated soil profiles. The four hypothetical cases are shown in Table 2.

The study by Anderson et al. (2004) first established benchmark solutions based on finite element studies from three organizations: Norwegian Geotechnical Institute (NGI), the Center for Offshore Foundation Systems (COFS) at the University of Western Australia, and the Offshore Technology Research Center (OTRC). The benchmark solutions were used to evaluate four simplified prediction methods: P1 (OTRC), P2 (COFS), P3 (NGI), and P4 (an industry predictor). The OTRC predictions utilized the simplified plastic limit analysis procedure for inclined loading conditions described earlier. Simplified solutions were compared to finite element solutions with regard to (1) anchor vertical holding capacity, (2) anchor horizontal capacity, (3) anchor capacity at intermediate load inclination angles, (4) optimal load attachment depth corresponding to maximum horizontal holding capacity, (5) load capacity for an anchor line attachment depth greater than optimum, and (6) load capacity for an anchor line attachment depth less than optimum.

The ratios of simplified analysis to finite element predictions are presented in Table 3. In all cases, the P1 (OTRC) simplified method predictions are always within 20% of the FEM benchmark values, and in most cases they are within 10%. Some of the larger differences between simplified and benchmark solutions were associated with vertical holding capacity estimates. This may be due in part to the idealized failure mechanism assumed in the development of this method, in which vertical side resistance and tip resistance are considered as two distinct, independent mechanisms. In actuality, some interaction occurs between these mechanisms, an effect that can be captured in finite element analyses but not in the simplified plasticity formulation.

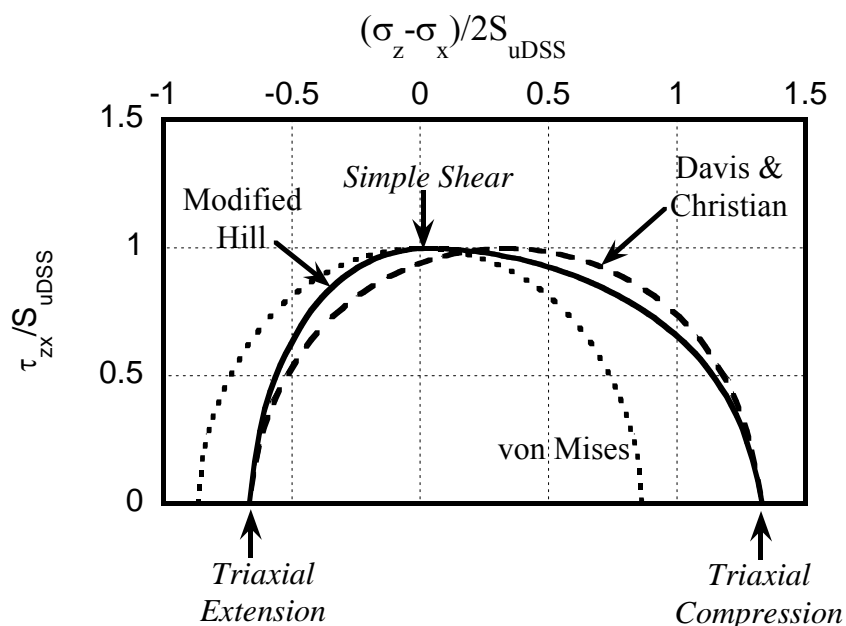


Figure 8. Anisotropic Yield Surfaces

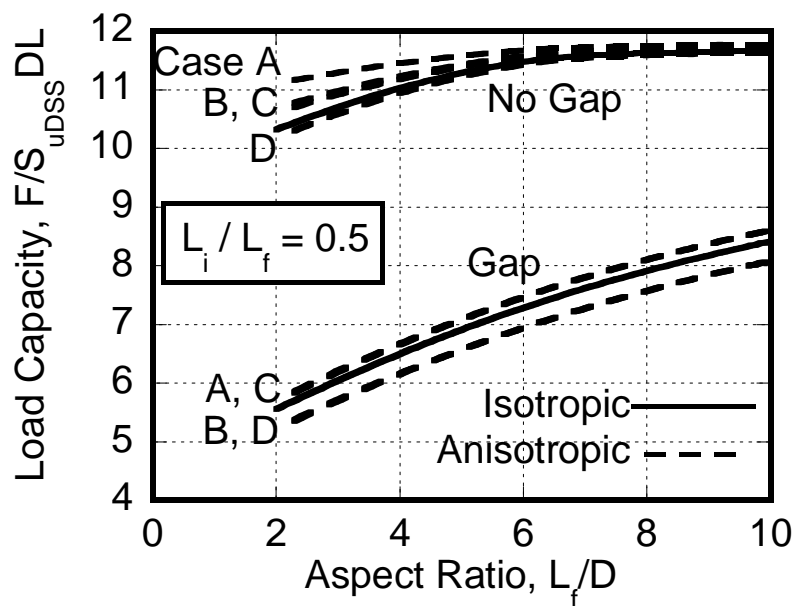


Figure 9. Influence of Strength Anisotropy on Predicted Suction Anchor Capacity

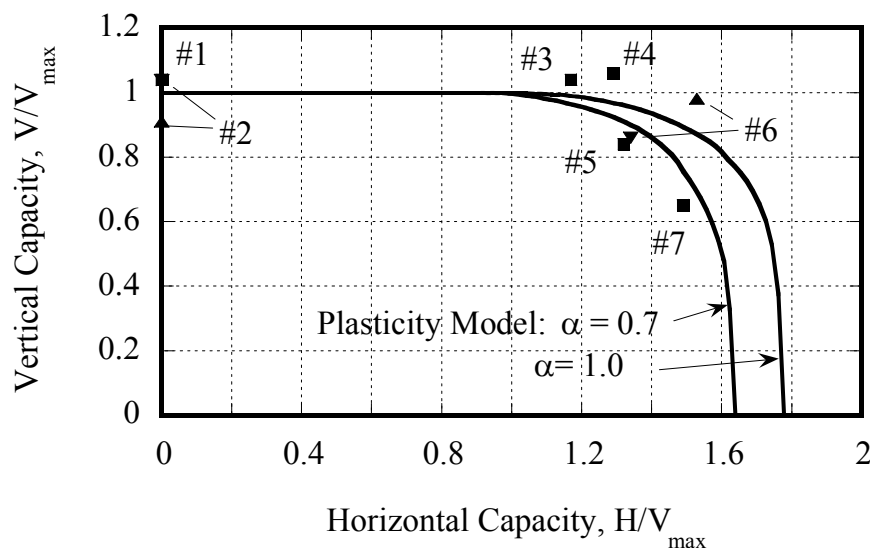


Figure 10. Load Capacity of Suction Anchors - Comparison of PLA Model Predictions to Centrifuge Test Results

Table 2. Geometry and Soil Profile Data for Studies Comparing Simplified Methods of Analysis to Finite Element Predictions (after Anderson et al., 2004).

Case	C1	C2	C3	C4
<b>Geometry</b>				
Outside Diameter	5m	5m	5m	5m
Target penetration depth	25m	7.5m	25m	7.5m
Depth/Diameter ratio	5	1.5	5	1.5
Structural model	Rigid cylinder with closed top			
Submerged weight	1100kN	330kN	1100kN	330kN
<b>Soil data</b>				
Overconsolidation ratio	1		~1.6	
$S_{uDSS}$	1.25z (kPa)		10kPa for $z < 5m$ 2z (kPa) for $z > 5m$	
$S_{uTC}$	1.2 $S_{uDSS}$			
$S_{uTE}$	0.8 $S_{uDSS}$			
$S_u$ vertical plane	$S_{uDSS}$			
Shear strength along outside skirt wall	0.65 $S_{uDSS}$			
$\sigma'_{vc}$	6z (kPa)		7.2z (kPa)	
$K_0$	0.55		1.0 ( $z < 5m$ ) 0.65 ( $z > 5m$ )	

Table 3. Ratio between capacity calculated by simplified methods and 3D finite element analyses (after Anderson et al., 2004).

CASE	Predictor	C1	C2	C3 no crack	C3 with crack	C4 no crack	C4 with crack
<b>Anchor <math>L_f/D</math>:</b>		<b>5</b>	<b>1.5</b>	<b>5</b>	<b>5</b>	<b>1.5</b>	<b>1.5</b>
<b>OCR:</b>		<b>1.0</b>	<b>1.0</b>	<b>~1.6</b>	<b>~1.6</b>	<b>~1.6</b>	<b>~1.6</b>
<b>Vertical capacity</b>	P1	0.98	0.83	0.98	1.20	0.86	0.99
	P2	0.88	0.85	0.87	0.85	0.88	0.90
	P3	0.94	0.93	0.93	1.00	0.97	1.03
	P4	0.98	0.82	0.89	0.89	0.67	0.68
<b>Horizontal capacity</b>	P1	0.95	1.03	0.95	1.09	1.03	0.99
	P2	0.98	1.19	0.97	1.11	1.14	0.99
	P3	0.95	0.89	0.95	1.03	0.89	0.87
	P4	0.97	0.98	0.98	1.03	0.85	0.85
<b>Capacity at intermediate load inclination, <math>\alpha</math></b>	$\alpha$	22.5/30°	45/60°	22.5/30°	22.5/30°	45/60°	45/60°
	P1	/0.97	1.01/0.98	/1.02	/1.18	1.01/0.89	1.06/1.06
	P2	/0.95	1.14/1.02	0.96/0.95	1.03/0.91	1.07/0.91	1.01/0.95
	P3	/0.97	0.91/1.00	0.97/1.00	1.05/0.95	0.98/0.98	0.96/1.03
	P4	/0.88	1.01/0.94	0.98/0.98	1.03/0.85	0.77/0.69	0.84/0.72
<b>Depth of optimum load attachment</b>	P1	1.01	1.01	1.02	1.02	1.00	1.02
	P2	1.06	1.01	1.02	1.00	1.00	1.02
	P3	1.01	1.01	1.02	1.00	1.00	1.00
	P4	1.03	1.03	1.02	1.00	1.08	1.05
<b>Attachment point below optimum</b>	P1	0.95	1.00	0.93	(1.09)	0.96	0.89
	P2	0.91	1.33	0.99	(1.09)	1.06	1.13
	P3	0.98	1.00	1.00	(1.20)	0.95	1.04
	P4	0.99	1.55	1.16	(1.00)	1.48	1.38
<b>Attachment point above optimum</b>	P1	1.04	0.92	1.10	1.18	0.96	0.99
	P2	1.06	1.10	1.08	1.01	1.14	0.99
	P3	0.90	0.95	0.98	0.91	0.92	1.01
	P4	0.78	0.89	1.03	1.05	0.75	0.80

Note: Predictor P1 = OTRC method.

Shading indicates the following:

Difference $\leq 10\%$	
Difference 10 to 20%	
Difference $>20\%$	

## PROGRESS AND RESULTS – VERTICALLY LOADED ANCHORS

Prediction of the holding capacity of vertically loaded anchors (VLA's) involves solving two major problems: (1) prediction of the trajectory of the anchor during drag embedment, and (2) estimation of the pullout capacity corresponding to the estimated embedment depth. The problems are actually somewhat inter-related, since prediction of the anchor trajectory requires a succession of estimates of collapse loads of the embedded anchor at various instants of time throughout the drag embedment process. The methodology for estimating the instantaneous collapse loads is essentially the same as that for estimating vertical pullout capacity, except that the re-positioning of the anchor must be taken into account for the vertical pullout capacity calculation. It should also be noted that the need for prediction of anchor trajectory during drag embedment is common to the drag embedment anchors (DEA's) used in conventional catenary mooring systems as well as VLA's. Hence, much of the analytical procedures and databases developed for DEA's are relevant to the VLA research effort.

### Analytical Approach

As with suction anchors, this research employs a general upper bound plasticity approach to estimating anchor trajectory and capacity. The discussion that follows presents the steps in the analysis for the case of an anchor with a rectangular fluke and a "thin" shank; i.e., the soil resisting force acting on the shank is negligible. Non-rectangular flukes and the effects of soil resistance on the shank can be modeled in the analysis; however, for clarity of presentation the discussion is restricted to relatively simple conditions.

#### *Plate Motions and Soil Resistance*

The anchor is modeled as a translating-rotating plate as shown in Figure 11. The soil resistance force parallel to the fluke  $F_s$  can be expressed in terms of soil undrained shear strength ( $S_u$ ), fluke length ( $L_f$ ), fluke width ( $w_f$ ), and a soil-anchor adhesion factor ( $\alpha$ ):

$$F_s = 2 S_u [\alpha L_f + N_{ps} w_f]$$

A reasonable estimate of the end bearing factor is  $N_{ps} = 12$ .

Characterizing soil resistance to rotation is somewhat more complex, since mobilized resistance is a function of the center of rotation of the fluke. Assuming uniform soil pressure acting on the fluke (Figure 12), the soil pressure  $q$  is related to undrained shear strength  $S_u$  by:

$$q = n_p S_u \quad (\text{Eq. 2a})$$

$$n_p = 6 + 6 d_c^2 / (L/2)^2 \quad (\text{Eq. 2b})$$

where  $d_c$  is the distance from the center of the fluke to the center of rotation, and  $L$  is the length of the fluke.

The bearing factor  $n_p$  will be a function of the center of rotation of the fluke motion. Solutions from plasticity theory suggest that the appropriate bearing factor for rotation about the center of the plate is  $n_p = 6$ , while for rotation about the edge of the plate  $n_p =$



12. As a trial solution for intermediate conditions of rotation between the above two conditions,  $n_p$  was assumed to vary as a second order function of distance of the center of rotation to the center of the fluke. A check on whether the above assumptions are reasonable is possible by considering resistance functions for the entire fluke:

$$V = N_p S_u L \quad (\text{Eq. 3})$$

$$M = N_m S_u L^2 / 4 \quad (\text{Eq. 4})$$

where  $V$  is the total soil resisting force acting normal to the long axis of the fluke,  $M$  is the soil resisting moment acting on the fluke, and  $N_p$  and  $N_m$  are dimensionless bearing factors. Figure 13 shows the interaction between  $N_p$  and  $N_m$  implied from Eq. 2. This interaction relationship is considered an acceptable solution in the sense that it is concave everywhere and satisfies the limiting conditions; i.e., for pure translation normal to the fluke  $N_p = 12$ , and for pure rotation about the center of the fluke  $N_p = 6$ .

### *Anchor Trajectory*

The section above considers the collapse load conditions under which the anchor will translate and rotate. This section discusses the framework for prediction of the anchor motions. Based on the soil resistance relationships presented above, an upper bound calculation can be performed to determine the collapse load  $F$  corresponding to an anchor line orientation  $\theta$  measured from horizontal. This process can be repeated to establish the relationship between  $F$  and  $\theta$  shown in Figure 14. The anchor line solution of Neubecker and Randolph (1996) in Figure 14 provides a locus of allowable anchor line tension forces and load attachment angles. The intersection of the two curves provides a unique point describing the orientation of the anchor at any point in the drag embedment process. With the anchor orientation thus determined at any time, the trajectory of the anchor is directly determined. This process is carried in steps where the anchor is assumed to rotate and translate in small increments. After each increment the calculation is repeated taking the anchor's new position into account.

### **Progress**

- The numerical algorithms for implementing a drag embedment model within the framework described above are largely completed. Remaining work in this area include: Evaluating the accuracy of the model and making refinements as needed.
- Parametric studies to investigate the effects of soil strength gradient and anchor geometry.
- Publication of results to obtain critical review and for dissemination of findings to practitioners.

### **FOCUS FOR 2004-2005**

Suction anchor studies are considered largely completed. Finalizing the VLA study will be the primary focus for 2004-2005.

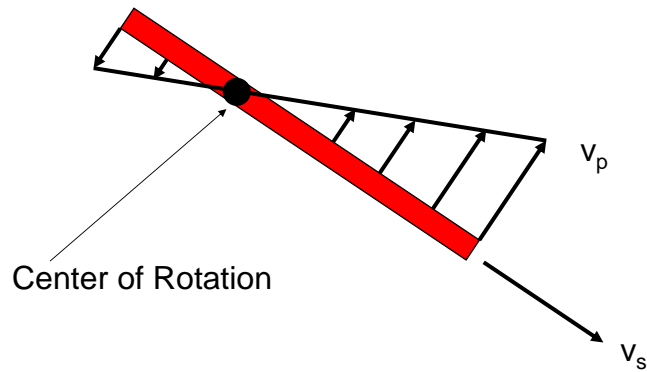


Figure 11. Kinematics of a Penetrating Anchor Fluke.

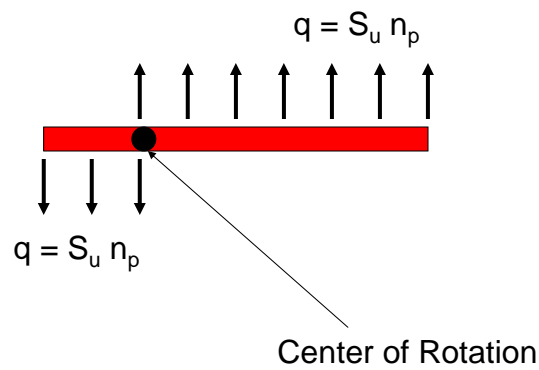


Figure 12. Soil Resistance to Fluke Rotation.

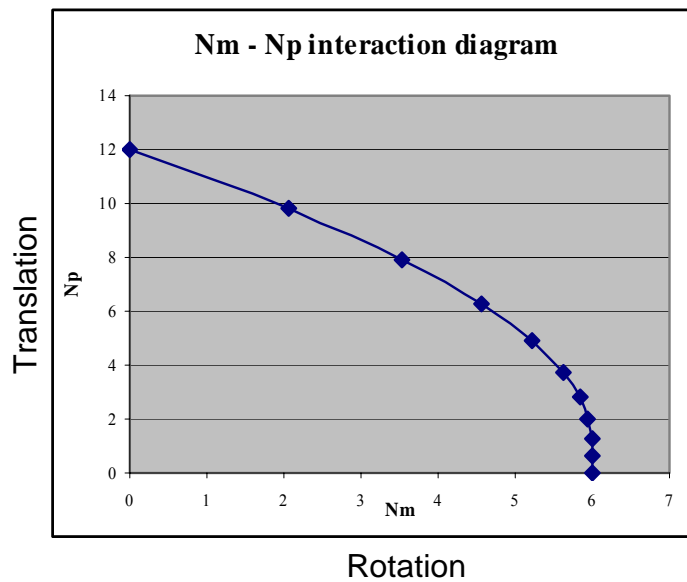


Figure 13. Interaction Diagram for Fluke Rotation-Translation

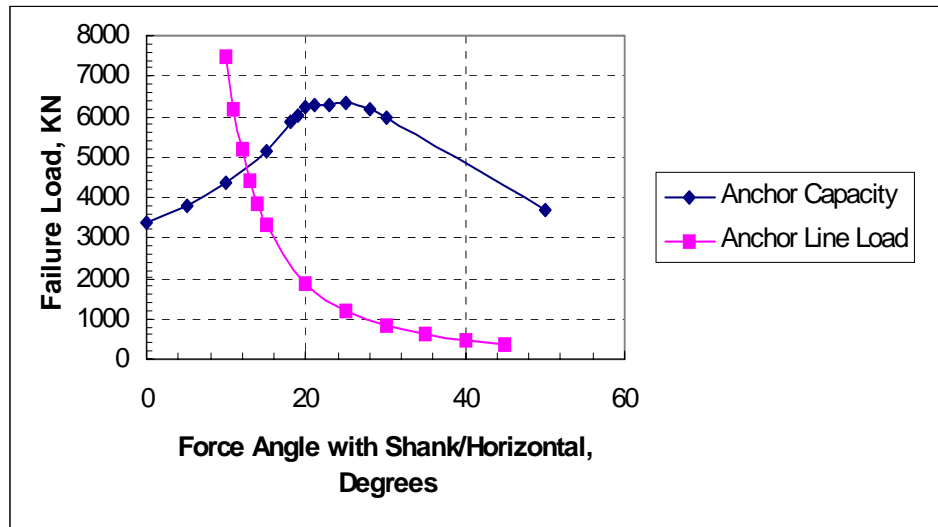


Figure 14. Force Angle and Anchor Line Curves

## REFERENCES

- Anderson, K.H., Murff, J.D., and Randolph, M. (2004) *Deepwater Anchor Design Practice*, Final Year Report submitted to the American Petroleum Institute and the Deepstar JIP.
- Aubeny, C.P. and Murff, J.D. (2004) "Simplified limit solutions for undrained capacity of suction anchors," *to be published in Journal of Ocean Engineering*.
- Aubeny, C.P., Han, S.W.\*, and Murff, J.D. (2003a) "Inclined load capacity of suction caisson anchors," *Intl. J. for Numerical and Analytical Methods in Geomechanics*, Vol. 27, pp. 1235-1254.
- Aubeny, C.P., Han, S.W. and Murff, J.D. (2003b) "Refined model for inclined load capacity of suction caissons," *22<sup>nd</sup> International Conference on Offshore and Arctic Engineering*, June 8-13, Cancun, Mexico, OMAE2003-37502.
- Aubeny C.P. Han S.W.\*, and Murff, J.D. (2003c) "Suction caisson capacity in anisotropic soil," *Intl. J. of Geomechanics*, Vol. 3, No. 4, pp. 225-235.
- Aubeny, C.P., Moon, S.K.\*, and Murff, J.D. (2001) "Lateral undrained resistance of suction caisson anchors," *Intl. J. Offshore and Polar Engineering*, Volume 11, No. 3, pp. 211-219.
- Clukey, E.C., Aubeny, C.P. and Murff, J.D. (2003) "Comparison of analytical and centrifuge model tests for suction caissons subjected to combined loads," *22<sup>nd</sup> International Conference on Offshore and Arctic Engineering*, June 8-13, Cancun, Mexico, OMAE2003-37503.
- Clukey, E. C. and Phillips, R. (2002) "Centrifuge Model Tests to Verify Suction Caisson Capacities for Taut and Semi-taut Legged Mooring Systems," *Proceedings of the Deep Offshore Technology Conference*, New Orleans.
- Davis, E.H. and Christian, J.T. (1971) "Bearing capacity of anisotropic cohesive soil," *ASCE J Soil Mech. and Found. Engr. Div*, **97**(SM5), pp. 753-769.
- Hill, R. (1950) *The Mathematical Theory of Plasticity*, Oxford University Press, London.

- Ladd, C.C. (1991) "Stability evaluation during staged construction," *ASCE J. Geotech. Engr.*; **117** (4), pp. 537-615.
- Matlock, H. (1970) "Correlations for design of laterally loaded piles in soft clay," *Proc. 2<sup>nd</sup> Offshore Tech. Conf.* Houston, pp. 577-594.
- Murff, J.D. (1980) "Vane shear testing of anisotropic, cohesive soils," *Intl. Journal for Numerical and Analytical Methods in Geomechanics*, **4**, pp.285-289.
- Murff, J.D. (1978) "Upper bound analysis of incompressible, anisotropic media," *Proc. 15<sup>th</sup> Annual Meeting of Engineering Science*, pp. 521-526.
- Murff J.D., and Hamilton J.M. (1993) "P-Ultimate for undrained analysis of laterally loaded piles," *ASCE Journal of Geotechnical Engineering*, **119** (1), pp. 91-107
- Neubecker, S.R. and Randolph, M.F. "Performance of embedded anchor chains and consequences for anchor design," *Marine Georesources and Technology*, Vol. 14, pp. 77-96.
- O'Neill, D.A. (1985) *Undrained strength anisotropy of an overconsolidated thixotropic clay*, MS Thesis, Dept. of Civ. And Envir. Engrg., MIT, Cambridge, Mass.
- Prager, W. (1959) *An Introduction to Theory of Plasticity*. Addison Wesley, Reading, Massachusetts.
- Randolph, M.F., and Houlsby, GT (1984) The limiting pressure on a circular pile loaded laterally in cohesive soil. *Geotechnique*, **34**(4), pp. 613-623.
- Randolph M.F. (2001) personal communication.
- Rauch A (2003) personal communication.
- Reese, LC, Cox, WR, and Koop, RD. (1975) "Field testing and analysis of laterally loaded piles in stiff clay," *Proc., 7<sup>th</sup> Offshore Tech. Conf.*, Houston, pp. 473-483.
- Whittle, A.J. and Aubeny, C.P. (1993) "The effects of installation disturbance on interpretation of in-situ tests in clays", *Predictive Soil Mech., Proc. of the Wroth Memorial Symp.*, Oxford, England, pp. 742-767.
- Wood, D.M. (1981) "True triaxial tests on Boston Blue Clay," *Proc., 10<sup>th</sup> Int. Conf. on Soil Mech. and Found. Engrg.*, pp. 825-830.